Journal of Materials Chemistry C

Solution-Processed Broadband Polymer Photodetectors with Spectral Response Up to 2.5 μm by a Low Bandgap Donor-Acceptor Conjugated Copolymer

Journal:	*Journal of Materials Chemistry C*
Manuscript ID	TC-ART-01-2018-000437.R2
Article Type:	Paper
Date Submitted by the Author:	27-Feb-2018

Complete List of Authors:	Zheng, Luyao; University of Akron Zhu, Tao; The University of Akron, polymer engineering Xu, Wenzhan; The University of Akron, polymer engineering Liu, Lei; The University of Akron Zheng, Jie; University of Akron, Chemical and Biomolecular Engineering Gong, Xiong; The University of Akron, Polymer Eng Wudl, Fred; UCSB, Department of Chemistry and Biochemistry 9510

Solution-Processed Broadband Polymer Photodetectors with Spectral Response Up to 2.5 μm by a Low Bandgap Donor-Acceptor Conjugated Copolymer

Luyao Zheng,[1#] Tao Zhu,[1#] Wenzhan Xu,[1] Lei Liu,[1] Jie Zheng,[3] Xiong Gong,[1*] and Fred Wudl[2*]

1) Department of Polymer Engineering, College of Polymer Science and Polymer Engineering, The University of Akron, Akron, OH 44325, USA

2) Department of Chemistry and Biochemistry, University of California, Santa Barbara, CA 93106

3) Department of Chemical & Bimolecular Engineering, The University of Akron, Akron, OH 44325, USA

Abstract

Photodetectors (PDs) with infrared (IR) response have extensive industrial and scientific applications. Broadband polymer PDs that operated at room temperature have drawn the greatest attentions in the past years. In this study, solution-processed polymer PDs with spectral response ranging from 350 nm to 2500 nm is reported. The low bandgap donor-acceptor (D-A) conjugated copolymer contributes to the IR photo-response. Implementation of bulk heterojunction device structure with polypyrrole as an interfacial layer to match the energy level of low bandgap D-A conjugated copolymer and Ba/Al bi-cathode to compress dark current gave rise to a large photocurrent to dark current ratio, which resulted in detectivities greater than 10^{11} Jones (1 Jones =1 $cmHz^{1/2}W^{-1}$) over the wavelength ranging from 350 nm to 2500 nm. Thus, our finding of utilization of bulk heterojunction composite consisting of a D-A low bandgap polymer blended with a fullerene derivative provides a facile way to detect IR radiation, indicating that broadband polymer PDs are a promising photoelectronic technology in the future.

#These authors are contributed to this work equally.

*Corresponding authors, e-mails: xgong@uakron.edu (XG), wudl@chem.ucsb.edu (FW); Fax: (330)9723406

1. Introduction

Photodetectors (PDs) with broadband spectral response have continuously drawn tremendous attention in the past decades due to their industrial and scientific applications. These applications include telecommunications, thermal imaging, chemical/biological sensing and spectroscopic and medical instruments.[1] Today, separate PDs or materials are required for different sub-bands within the ultraviolet (UV)-visible to infrared (IR) range.[1] Traditional InCaAs- and HgCdTe-based IR PDs require extremely low operation temperature, and need to be operated at high voltage to obtain reasonable detectivity,[2,3] which limited their applications in biosensor and image sensors where low operation voltage is required. In addition, expensive manufacturing processes are required to fabricate these IR PDs. Recently, colloidal quantum dots (QDs), such as PbS and HgTe, were comprehensively studied to demonstrate IR PDs.[4-7] But a planar device structure was used for fabrication of colloidal QDs based IR PDs, where high operation voltage was also required to receive a decent detectivity even if these IR PDs can be operated at room temperature. More recently, two-dimensional (2D) graphene and transition metal dichalcogenides, as alternative candidates, were shown to address long wavelength region detection with high resolution arising from their novel nanoscale structures, rich physics and high mobility.[8-11] But the small-scale and uncertain fabrication of mono- and multi-layer 2D materials as well as the high gate (or drive) voltages to be used for thin film transistors restricted their further applications.

In contrast to inorganic PDs, polymer PDs have captured abundant research interest owning to their ease of processing, low cost, physical flexibility and remarkable detectivity over broadband spectral response since the discovery of ultrafast photo-induced electron transfer from conjugated polymers to fullerenes.[12-15] Utilizing a low bandgap donor-acceptor (D-A) conjugated

copolymer, such as polythieno[3,4-*b*]thiophene (PTT), excellent ultraviolet (UV)-visible to near IR (NIR) detection was reported.[16] Later on, the photoresponsivity of polymer PDs was successfully extended to 1450 nm with detectivity greater than 10^{12} Jones (1 Jones =1 $cmHz^{1/2}W^{-1}$) under low bias, implementing optimal photodiode structure, based on poly(5,7-bis(4-decanyl-2-thienyl)-thieno(3,4-*b*)diathiazole-thiophene-2,5) (PDDTT):(6,6)-phenyl-C_{61}-butyric acid methyl ester ($PC_{61}BM$) bulk heterojunction (BHJ) composite.[17] To further extend spectral response, various new moleculars were developed,[18-23] for example, a novel donor unit dithienobenzotrithiophen (DTBTT) was utilized to create D-A polymers with the thienoisoindigo-based acceptor.[18] On the other hand, various technologies including three-phase morphology evolution,[24] the interfacial layer engineering,[25-28] molecular engineering,[29] adjustment of molecular arrangement,[30] have been used to enhance the detectivities of polymer PDs. However, there is no report on polymer PDs with detection beyond 1600 nm.[18]

In this study, we report polymer PDs with a detectivity greater than 10^{11} Jones over the wavelength ranging from 350 nm to 2500 nm, through a BHJ photodiode structure composing of a low bandgap D-A copolymer, poly[(4,7-bis(3-hexylthien-2-yl)-2 λ ^{4} δ ^{2}-benzo[1,2-c;4,5c']bis[1,2,5]thiadiazole)-alt-(N-(3,4,5-tris(dodecyloxy)phenyl)-dithieno[3,2-b:2',3'-d]pyrrole)] (PBBTPD), blended with a fullerene derivative, tri-phenyl-C_{61}-butyric acid methyl ester (Tri-$PC_{61}BM$). This is the first report on polymer PDs which exhibit a photoresponse up to 2.5 μm.

2. Experimental Section

2.1. Materials

The synthesis of PBBTPD was reported elsewhere.[31,32] The synthesis of Tri-$PC_{61}BM$ was also reported elsewhere.[33,34] Polypyrrole (PPy) was obtained from Aldrich and used as received

without further treatment.

2.2. Preparation and characterization of thin films

The thin films of PBBTPD, Tri-$PC_{61}BM$ and the PBBTPD:Tri-$PC_{61}BM$ BHJ composite were spin-coated on the top of quartz subtracts from corresponding toluene solutions for absorption spectroscopy measurement. The absorption spectra measurement was conducted in air. The film thickness was measured on the DektakXT surface profile measuring system. Atom force microscopy (AFM) images were conducted on Brucker AXS, with the tapping mode. The roughnesses of the samples were analyzed using Nanoscope Analysis software. For ultraviolet photoelectron spectroscopy (UPS**)** measurements, a 100 nm thick Au film was deposited on pre-cleaned Si substrates with a thin native oxide. The PBBTPD thin film, which is prepared from toluene solution by spin-casting, was fabricated inside a nitrogen atmosphere glovebox and was transferred via an airtight sample holder to the UPS analysis chamber. The sample was also kept in a high vacuum chamber overnight to remove solvent residues. The UPS analysis chamber was equipped with a hemispherical electron energy analyzer (Kratos Ultra Spectrometer) and was maintained at 1×10^{-9} Torr. The UPS measurement was carried out using a He I ($h\nu$=21.2eV) source. During UPS measurement, a sample bias of -9 V was used in order to separate the sample and the secondary edge the analyzer.

2.3. Fabrication and characterization of polymer photodetectors

The pre-cleaned ITO (indium tin oxide) substrates were treated by UV ozone plasma for 20 minutes (mins) in ambient atmosphere. After that, a ~ 40 nm thick PPy thin layer was spin-coated onto the ITO-coated glass, followed by thermal annealing at 120°C for 20 mins in air. Afterward, the PPy-coated ITO substrates were immediately transferred into a glovebox with a nitrogen atmosphere. When the PPy-coated ITO substrates were cooled down to room-

temperature, ~ 120 nm thick PBBTPD:Tri-$PC_{61}BM$ BHJ composite thin film was spin-coated on the top of the PPy-coated ITO substrates from PBBTPD:Tri-$PC_{61}BM$ (the ratio of PBBTPD to Tri-$PC_{61}BM$ is 1:2 by weight) toluene solution. The films were then thermally annealed at different temperatures (60 ^{o}C, 80 °C and 100 ^{o}C) for 30 mins. Finally, a ~5 nm of Barium (Ba) and a 150 nm Aluminum (Al) films were thermally deposited through a shadow mask under a vacuum of 1×10^{-6} mbar. The device areas were measured to be 0.045 cm^2.

The current density-voltage (J-V) characteristics of polymer PDs were obtained by using a Keithley model 2400 source measurement unit. A Newport Air Mass 1.5 Global (AM1.5G) full-spectrum solar simulator was applied as the light source. The light intensities for white light were 100 mW cm^{-2}, for the wavelength (λ) of 800 nm was 0.22 mW cm^{-2} and for λ=1500 nm was 0.05 mW cm^{-2}.

3. Results and Discussion

The molecular structure of PBBTPD is shown in **Figure 1a.** PBBTPD consists of a strong accepting moiety benzobisthiadiazole and donating moiety dithienopyrrole along the polymer chain. The lowest unoccupied molecular orbitals (LUMO) of benzobisthiadiazole is around 4.1 eV below the vacuum owing to the high electron affinity.[31] Together with the strong electron donating moiety dithienopyrrole, the resulting D-A polymer, PBBTPD, would exhibit a very low optical band gap.[35,36] Figure 1b displays the molecular structure of Tri-$PC_{61}BM$, which is used for fabrication of polymer PDs. **Figure 1c** presents the absorption spectrum of PBBTPD thin film. There are two prominent absorption peaks in the wavelength range from 300 nm to 2500 nm. One located at ~ 510 nm originates from the π-π^* transition of the donating moiety,[35,37] while the other one located at ~ 1200 nm is attributed to the donor-to-acceptor charge-transfer band.[36] In addition, the optical band gap of PBBTPD thin film is estimated to be 0.50 eV

corresponding to the absorption edge at 2500 nm. The ultrabroad absorption of PBBTPD thin film indicates that polymer PDs fabricated with PBBTPD thin film have a potential of detection from the UV-vis to the IR region.

Figure 2 shows the UPS spectra of PBBTPD thin film. The abscissa is the binding energy relative to the Fermi energy (E_F) of Au, which is defined by the energy of the electron before excitation relative to the vacuum level. **Figure 2a** shows the high binding energy cutoff (E_{cutoff}) of PBBTPD thin film; E_{cutoff} is determined by linear extrapolation to zero of the yield of secondary electrons. From **Figure 2a**, E_{cutoff} = 17.13±0.03 eV for PBBTPD thin film. **Figure 2b** shows the HOMO region (0-4 eV) for PBBTPD thin film. The HOMO energy is determined using the incident photon energy, hv = 21.2 eV, E_{cutoff}, and the E_{onset} (the onset of PBBTPD thin film relative to the E_F of Au). From the data in **Figure 2b**, E_{onset} = 0.19±0.03eV for PBBTPD thin film. The HOMO energy is thus obtained directly from the UPS measurement,

$$E_{HOMO} = hv - (E_{cutoff} - E_{onset})^{38,39} \qquad (1)$$

For PBBTPD thin film, E_{HOMO} = -4.26±0.06 eV. The LUMO energy is calculated using the HOMO levels and the optical gaps (E_g) obtained from UV-Vis absorption spectra shown in **Figure 1c**. Thus, the E_{LUMO} = -3.71±0.06 eV is for PBBTPD thin film.

In order to approach high photocurrent from polymer PDs, BHJ composite of PBBTPD blended with Tri-$PC_{61}BM$ thin film is used as the active layer.[17] As compared with the LUMO energy level of either $PC_{61}BM$ or $PC_{71}BM$, Tri-$PC_{61}BM$ possesses a higher LUMO energy level,.[33,34] which creates a large energy difference with the HOMO energy of PBBTPD, resulting in low dark current, based on photodiode properties.[17] The absorption spectra of Tri-$PC_{61}BM$ thin film and PBBTPD:Tri-$PC_{61}BM$ BHJ composite thin film are displayed in **Figure 1c**. It is clear that the absorption of PBBTPD:Tri-$PC_{61}BM$ BHJ composite thin film is super-position of

PBBTPD thin film and Tri-$PC_{61}BM$ thin film, ranging from 300 nm and 2500 nm. Certainly, Tri-$PC_{61}BM$ thin film contributes absorption from 300 nm to 500 nm.

It was well-known that the film morphology of BHJ composite active layer plays significant role in the device perfroamnce.[40] Towards the end, the film morphology of PBBTPD:Tri-$PC_{61}BM$ composite layer annealed at different temperature is firstly studied. The AFM height and phase images of BHJ composite layer annealed at temperatures of 60 □, 80 □, and 100 □ are shown in **Figure 3**. It is found that the root mean square (RMS) of BHJ composite layer annealed at temperatures of 60 □, 80 □, and 100 □ possesses RMS values of 0.877 nm, 0.457 nm and 0.545 nm, respectively. The smaller RMS value indicates BHJ composite layer possesses smoother surface, which is favorable for charge carrier to be transported and collected by the electrode.[40] In addition, it is found that BHJ composite layer annealed at the temperature of 60 □ possesses a dramatically phase separation, which is unfavorable for charge carrier dissociation. The pronounced pinholes and defects are observed from BHJ composite layer annealed at the temperature of 100 □. These pinholes and defects would restrict separated charge carriers to be transported to the corresponding electrodes. Whereas, a homogenous phase separation is observed from BHJ composite layer annealed at the temperature of 80 □. Thus, better device performance is anticipated from the polymer PDs where BHJ composite layer is annealed at the temperature of 80 □.

Figure 4a presents the device structure of polymer PDs. The work functions of ITO, PPy, Ba, and Al, and the HOMO and LUMO energy levels of PBBTPD thin film and Tri-$PC_{61}BM$ thin film are shown in **Figure 4b**. PPy rather than PEDOT:PSS (poly(3,4-ethylenedioxythiophene) polystyrene sulfonate) is used as a hole extraction interface layer because of the good energy match between the HOMO energy level of PPy thin film and the HOMO energy level of

PBBTPD thin film.[41] As indicated in **Figure 4b**, both HOMO and LUMO energy offsets between PBBTPD and Tri-$PC_{61}BM$ are larger than 0.30 eV, which indicates that efficient charge transfer between PBBTPD and Tri-$PC_{61}BM$ under illumination would take place.[42,43]

Figure 5a presents J-V characteristics of polymers PDs with either Al cathode or the Ba/Al bilayer cathode. The Ba/Al bilayer electrode is used for boosting device performance, in term of enhanced photocurrent and reduced dark current. By utilization of the low work function of Ba, an upward dipole would be formed between Tri-$PC_{61}BM$ thin film and Ba electrode.[44,45] As a result, the energy offset between the LUMO energy level of Tri-$PC_{61}BM$ and the HOMO energy level of PBBTPD would be enlarged, resulting in reduced dark current densities for polymer PDs.[43,45] As expected, the polymer PDs with the Ba/Al bilayer electrode exhibits low darkcurrent densities. Thus boosted detectivity is anticipated from polymer PDs with the Ba/Al bilayer electrode.[17,46]

The J-V characteristics of polymer PDs with the Ba/Al bilayer cathode illuminated with white light (with a light intensity of 100 mW cm^{-2}), a monochromatic light of wavelength (λ) of 800 nm (with a light intensity of 0.22 mW cm^{-2}), and a monochromatic light at λ=1500 nm (with a light intensity of 0.05 mW cm^{-2}) and in dark are shown in **Figure 5b**. In dark, the J-V characteristic shows the rectification behavior which indicates the asymmetric characteristics of polymer PDs. The ratios of photocurrent to dark current are in the magnitude of 10^4, 10^3 and 10^2 for polymer PDs under white light illumination, a monochromatic light at λ =800 nm, a monochromatic light λ=1500 nm, respectively. These results confirm that charge carrier can be efficiently generated, separated and transferred within BHJ PBBTPD:Tri-$PC_{61}BM$ composite and then being collected by two different electrodes.[12,47]

The projected detectivity D^* is estimated by

$$D^* = (\frac{J_{ph}}{L_{light}})/(2qJ_d)^{1/2} \quad (2)$$

(where J_{ph} is photocurrent density, L_{light} is the light intensity, the q is the absolute value of electron charge (1.6×10^{-19} Coulombs) and J_d is the dark current).[17] Biased at -1.0 V, polymer PDs exhibits the detectivities of 1.39×10^{11} Jones at λ=800 nm and 2.20×10^{11} Jones at λ=1500 nm.

Figure 6 shows the external quantum efficiency spectrum of polymer PDs. Due to the limitation of the instrument, polymer PDs under our investigation only presents spectral response up to 1700 nm. In **Figure 6**, two data points, i.e. the detectivities of polymer PDs at wavelengths of 800 nm and 1500 nm are also added. These detectivities are calculated ones according to equ. (2), where J_{ph} and J_d are measured current densities. **Table 1** summarizes the photocurrent density, dark current density, on/off ratio, EQE, responsivity, and detectivity of polymer PDs. Moreover, it is found that the detectivities at wavelengths of 800 nm and 1500 nm are consistent very well with the estimated detectivities based on the EQE spectrum. Thus, the detectivities versus wavelength ranging 350 nm to 2500 nm are estimated based on the absorption spectrum of BHJ PBBTPD:Tri-$PC_{61}BM$ composite, and the results are shown in **Figure 6**. Therefore, operated at room temperature, polymer PDs presents the detectivities greater than 10^{11} Jones from 350 nm to 2500 nm.

4. Conclusion

Solution-processed polymer PDs based on PBBTPD:Tri-$PC_{61}BM$ BHJ composites and optimal band alignment of the vertical photodiode structure, with spectral response ranging from 350 nm to 2500 nm was demonstrated. The low bandgap D-A copolymer, PBBTPD, contributes to the IR photo-response even extended to 2500 nm. Implementation of photodiode structure with PPy interfacial layer and Ba/Al bi-cathode gave rise to the photocurrent to dark current ratio

resulting in the detectivities greater than 10^{11} Jones over the wavelength region from 350 nm to 2500 nm under low applied bias. Thus, our finding of utilization of a D-A low bandgap polymer blended with fullerene derivative in a vertical photodiode provides a facile way to detect IR radiation, which indicates that broadband polymer PDs are promising photoelectronic technology in the further.

Acknowledgements

XG acknowledges Professor Fred Wudl for his great encouragement and also celebrates his greatest contributions in the field of organic semiconductors and their applications for 50 years. The authors at The University of Akron acknowledge National Science Foundation (EECS 1351785) and Air Force Office of Scientific Research (Grant Number: FA9550-15-1-0292, Program Manager: Dr. Kenneth Caster) for financial support and Dr. Rajeev Kumar for assistance with materials development. TZ thanks Miss Xiaoteng Wang for assistance with AFM measurements.

References

1) Jha, A. R.; Jha, A.; Jha, D. A., *IR technology: applications to electrooptics, photonic devices, and sensors*. Wiley New York: **2000**.

2) Rogalski, A., HgCdTe IR detector material: history, status and outlook. *Reports on Progress in Physics* **2005,** *68* (10), 2267.

3) Olsen, G. H.; Joshi, A. M.; Ban, V. S. In *Current status of InGaAs detector arrays for 1-3 μm*, IR Technology XVII, International Society for Optics and Photonics: **1991**; pp 596-606.

4) Konstantatos, G.; Howard, I.; Fischer, A.; Hoogland, S.; Clifford, J.; Klem, E.; Levina, L.; Sargent, E. H., Ultrasensitive solution-cast quantum dot photodetectors. *Nature* **2006,** *442* (7099), 180-183.

5) Keuleyan, S.; Lhuillier, E.; Brajuskovic, V.; Guyot-Sionnest, P., Mid-IR HgTe colloidal quantum dot photodetectors. *Nature Photonics* **2011,** *5* (8), 489-493.

6) McDonald, S. A.; Konstantatos, G.; Zhang, S.; Cyr, P. W.; Klem, E. J.; Levina, L.; Sargent, E. H., Solution-processed PbS quantum dot IR photodetectors and photovoltaics. *Nature materials* **2005,** *4* (2), 138-142.

7) Konstantatos, G.; Sargent, E. H., Colloidal quantum dot photodetectors. *IR Physics & Technology* **2011,** *54* (3), 278-282.

8) Xia, F.; Mueller, T.; Lin, Y.-m.; Valdes-Garcia, A.; Avouris, P., Ultrafast graphene photodetector. *Nature nanotechnology* **2009,** *4* (12), 839-843.

9) Liu, C.-H.; Chang, Y.-C.; Norris, T. B.; Zhong, Z., Graphene photodetectors with ultra-broadband and high responsivity at room temperature. *Nature nanotechnology* **2014,** *9*

(4), 273-278.

10) Zhang, K.; Zhang, T.; Cheng, G.; Li, T.; Wang, S.; Wei, W.; Zhou, X.; Yu, W.; Sun, Y.; Wang, P., Interlayer transition and IR photodetection in atomically thin type-II MoTe2/MoS2 van der Waals heterostructures. *ACS nano* **2016,** *10* (3), 3852-3858.

11) Xie, Y.; Zhang, B.; Wang, S.; Wang, D.; Wang, A.; Wang, Z.; Yu, H.; Zhang, H.; Chen, Y.; Zhao, M., Ultrabroadband MoS_2 Photodetector with Spectral Response from 445 to 2717 nm. *Advanced Materials* **2017,** *29* (17).

12) Sariciftci, N. S.; Smilowitz, L.; Heeger, A. J.; Wudl, F., Photoinduced electron transfer from a conducting polymer to buckminsterfullerene. *Science* **1992**, 1474-1476.

13) Yu, G.; Gao, J.; Hummelen, J. C.; Wudl, F.; Heeger, A. J., Polymer photovoltiac cells: Enhanced efficiencies via a network of internal donor-acceptor heterojunctions. *Science* **1995,** *270* (5243), 1789.

14) Schilinsky, P.; Waldauf, C.; Brabec, C. J., Recombination and loss analysis in polythiophene based bulk heterojunction photodetectors. *Applied Physics Letters* **2002,** *81* (20), 3885-3887.

15) O'Brien, G. A.; Quinn, A. J.; Tanner, D. A.; Redmond, G., A single polymer nanowire photodetector. *Advanced Materials* **2006,** *18* (18), 2379-2383.

16) Yao, Y.; Liang, Y.; Shrotriya, V.; Xiao, S.; Yu, L.; Yang, Y., Plastic Near□IR Photodetectors Utilizing Low Band Gap Polymer. *Advanced Materials* **2007,** *19* (22), 3979-3983.

17) Gong, X.; Tong, M.; Xia, Y.; Cai, W.; Moon, J. S.; Cao, Y.; Yu, G.; Shieh, C.-L.; Nilsson, B.; Heeger, A. J., High-detectivity polymer photodetectors with spectral response from 300 nm to 1450 nm. *Science* **2009,** *325* (5948), 1665-1667.

18) Han, J. F.; Qi, J.; Zheng, X. P.; Wang, Y. K.; Hu, L. Y.; Guo, C.; Wang, Y.; Li, Y. N.; Ma, D. G.; Qiao, W. Q.; Wang, Z. Y., Low-bandgap donor-acceptor polymers for photodetectors with photoresponsivity from 300 nm to 1600 nm, J. Mater. Chem. C: **2017**, 5, 159-165.

19) Hu, L. Y.; Han, J. F.; Qiao, W. Q.; Zhou, X. K.; Wang, C. L; Ma, D. G.; Li, Y. N.; Wang, Z. Y., Side-chain engineering in naphthalenediimide-based n-type polymers for high-performance all-polymer photodetectors, Polymer Chemistry, **2018**, 9, 327-334.

20) Hu, L. Y.; Qiao, W. Q.; Zhou, X. K.; Han, J. F.; Zhang, X. Q.; Ma, D. G.; Li, Y. N.; Wang, Z. Y., Side-chain engineering for fine-tuning of molecular packing and nanoscale blend morphology in polymer photodetectors, Polymer Chemistry, **2017**, 8, 2055-2062.

21) Hu, L.Y; Qiao, W. Q.; Han, J. F.; Zhou, X. K.; Wang, C. L.; Ma, D. G.; Wang, Z. Y.; Li, Y. N., Naphthalene diimide-diketopyrrolopyrrole copolymers as non-fullerene acceptors for use in bulk-heterojunction all-polymer UV-NIR photodetectors, Polymer Chemistry, **2017**, 8, 528-536.

22) Wang, X. F.; Lv, L.; Li, L. L.; Chen, Y. S.; Zhang, K.; Chen, H. R.; Dong, H. L.; Huang, J. S.; Shen, G. Z.; Yang, Z.; Huang, H., High-Performance All-Polymer Photoresponse Devices Based on Acceptor-Acceptor Conjugated Polymers, Adv. Funct. Mater., **2016**, 26,6306-6315.

23) Yao, B.; Zhou, X. K.; Ye, X. C.; Zhang, J.; Yang, D. Z.; Ma, D. G.; Wan, X. H., 2,1,3-Benzothiadiazole-5,6-dicarboxylic imide based low-bandgap polymers for solution processed photodiode application, Organic Electronics, **2015**, 26, 305-313.

24) Wang, H. Y.; Xing, S.; Zheng, Y. F; Kong, J. M.; Yu, J. S.; Taylor, A. D., Three-Phase Morphology Evolution in Sequentially Solution-Processed Polymer Photodetector:

Toward Low Dark Current and High Photodetectivity, ACS Appl. Mater. Interf. **2018**, 10, 3856-3864.

25) Zhou, X. K.; Yang, D. Z.; Ma, D. G.; Vadim, A.; Ahamad, T.; Alshehri, S. M., Ultrahigh Gain Polymer Photodetectors with Spectral Response from UV to Near-Infrared Using ZnO Nanoparticles as Anode Interfacial Layer, Adv. Funct. Mater., **2016**, 26, 6619-6626.

26) Hu, X. W.; Wang, K.; Liu, C.; Meng, T. Y.; Dong, Y.; Liu, S. J.; Huang, F.; Gong, X.; Cao, Y., High-detectivity inverted near-infrared polymer photodetectors using cross-linkable conjugated polyfluorene as an electron extraction layer, J. Mater. Chem. C., **2014**, 2, 9592-9598.

27) Sato, Y.; Kajii, H.; Ohmori, Y., Improved performance of polymer photodetectors using indium-tin-oxide modified by phosphonic acid-based self-assembled monolayer treatment, Organic Electronics, **2014**, 15,1753-1758.

28) Liu, X. L.; Zhou, J. J.; Zheng, J.; Becker, M. L.; Gong, X., Water-soluble CdTe quantum dots as an anode interlayer for solution-processed near infrared polymer photodetectors, Nanoscale **2013**, 5, 12474-12479

29) Zhang, L. Z.; Yang, T. B.; Shen, L.; Fang, Y. J.; Dang, Li; Z., N. J.; Guo, X.; Hong, Z. R.; Yang, Y.; Wu, H. B.; Huang, J. S.; Liang, Y. Y., Toward Highly Sensitive Polymer Photodetectors by Molecular Engingineering, Adv. Mater., **2015**, 27, 6496-6503.

30) Wang, W. B.; Zhang, F. J. Li, L. L.; Gao, M.; Hu, B., Improved Performance of Photomultiplication Polymer Photodetectors by Adjustment of P3HT Molecular Arrangement, ACS Appl. Mater. Interf., **2015**, 7, 22660-22668.

31) Yuen, J. D.; Kumar, R.; Zakhidov, D.; Seifter, J.; Lim, B.; Heeger, A. J.; Wudl, F.,

Ambipolarity in Benzobisthiadiazole□Based Donor–Acceptor Conjugated Polymers. *Advanced Materials* **2011,** *23* (33), 3780-3785.

32) Yuen, J. D.; Wang, M.; Fan, J.; Sheberla, D.; Kemei, M.; Banerji, N.; Scarongella, M.; Valouch, S.; Pho, T.; Kumar, R., Importance of unpaired electrons in organic electronics. *J. Polymer Science Part A: Polymer Chemistry* **2015,** *53* (2), 287-293.

33) Gong, X.; Yu, T.; Cao, Y.; Heeger, A. J., Large open-circuit voltage polymer solar cells by poly (3-hexylthiophene) with multi-adducts fullerenes. *Science China Chemistry* **2012,** *55* (5), 743-748.

34) Lenes, M.; Shelton, S. W.; Sieval, A. B.; Kronholm, D. F.; Hummelen, J. C. K.; Blom, P. W., Electron trapping in higher adduct fullerene□based solar cells. *Advanced Functional Materials* **2009,** *19* (18), 3002-3007.

35) Steckler, T. T.; Zhang, X.; Hwang, J.; Honeyager, R.; Ohira, S.; Zhang, X.-H.; Grant, A.; Ellinger, S.; Odom, S. A.; Sweat, D., A spray-processable, low bandgap, and ambipolar donor− acceptor conjugated polymer. *Journal of the American Chemical Society* **2009,** *131* (8), 2824-2826.

36) Zhang, X.; Steckler, T. T.; Dasari, R. R.; Ohira, S.; Potscavage, W. J.; Tiwari, S. P.; Coppée, S.; Ellinger, S.; Barlow, S.; Brédas, J.-L., Dithienopyrrole-based donor–acceptor copolymers: low band-gap materials for charge transport, photovoltaics and electrochromism. *Journal of Materials Chemistry* **2010,** *20* (1), 123-134.

37) Zhang, J.; Cai, W.; Huang, F.; Wang, E.; Zhong, C.; Liu, S.; Wang, M.; Duan, C.; Yang, T.; Cao, Y., Synthesis of quinoxaline-based donor− acceptor narrow-band-gap polymers and their cyclized derivatives for bulk-heterojunction polymer solar cell applications. *Macromolecules* **2011,** *44* (4), 894-901.

38) Gong, X.; Tong, M.; Brunetti, F. G.; Seo, J.; Sun, Y.; Moses, D.; Wudl, F.; Heeger, A. J., Bulk Heterojunction Solar Cells with Large Open□Circuit Voltage: Electron Transfer with Small Donor□Acceptor Energy Offset. *Advanced Materials* **2011,** *23* (20), 2272-2277.

39) Sun, Y.; Takacs, C. J.; Cowan, S. R.; Seo, J. H.; Gong, X.; Roy, A.; Heeger, A. J., Efficient, Air□Stable Bulk Heterojunction Polymer Solar Cells Using MoOx as the Anode Interfacial Layer. *Advanced materials* **2011,** *23* (19), 2226-2230.

40) Heeger, A. J.; Sariciftci, N. S.; Namdas, E. B., Semiconducting and metallic polymers, Oxford University Press, **2010**, p214-249.

41) Thompson, B. C.; Fréchet, J. M., Polymer–fullerene composite solar cells. *Angewandte chemie international edition* **2008,** *47* (1), 58-77.

42) Servaites, J. D.; Ratner, M. A.; Marks, T. J., Organic solar cells: a new look at traditional models. *Energy & Environmental Science* **2011,** *4* (11), 4410-4422.

43) Hendriks, K. H.; Li, W.; Wienk, M. M.; Janssen, R. A., Small-bandgap semiconducting polymers with high near-IR photoresponse. *Journal of the American Chemical Society* **2014,** *136* (34), 12130-12136.

44) Yu, G., Gao, J., Hummelen, J. C., Wudl, F. & Heeger, A. J. Polymer photovoltiac cells: Enhanced efficiencies via a network of internal donor-acceptor heterojunctions. *Science* **270**, 1789 (1995).

45) Crispin, X., Geskin, V., Crispin, A., Cornil, J., Lazzaroni, R., Salaneck, W. R., & Bredas, J. L. Characterization of the interface dipole at organic/metal interfaces. *Journal of the American Chemical Society* **124**, 8131-8141 (2002).

46) Hung, L., Tang, C. W. & Mason, M. G. Enhanced electron injection in organic

electroluminescence devices using an Al/LiF electrode. *Applied Physics Letters* **70**, 152-154 (1997).

47) Lee, C.; Yu, G.; Moses, D.; Pakbaz, K.; Zhang, C.; Sariciftci, N.; Heeger, A.; Wudl, F., Sensitization of the photoconductivity of conducting polymers by C 60: Photoinduced electron transfer. *Physical Review B* **1993,** *48* (20), 15425.

Table 1 Device performance paramters of polymer PDs

Peroformance paramters	Dark Currnt Density (J_d) (mA/cm^2)	Photocurrent Density (J_{ph}) (mA/cm^2)	J_{ph}/J_d	EQE (%)	Responsivity (R) (mA/W)	Detectivity (Jones)
at 800 nm and -0.5 V	**1×10^{-6}**	**1×10^{-5}**	**10**	**8.4**	**5×10^{-2}**	**1.4×10^{11}**
at 1500 nm and -0.5 V	**1×10^{-6}**	**7×10^{-6}**	**7**	**13.4**	**1.4×10^{-4}**	**2.2×10^{11}**

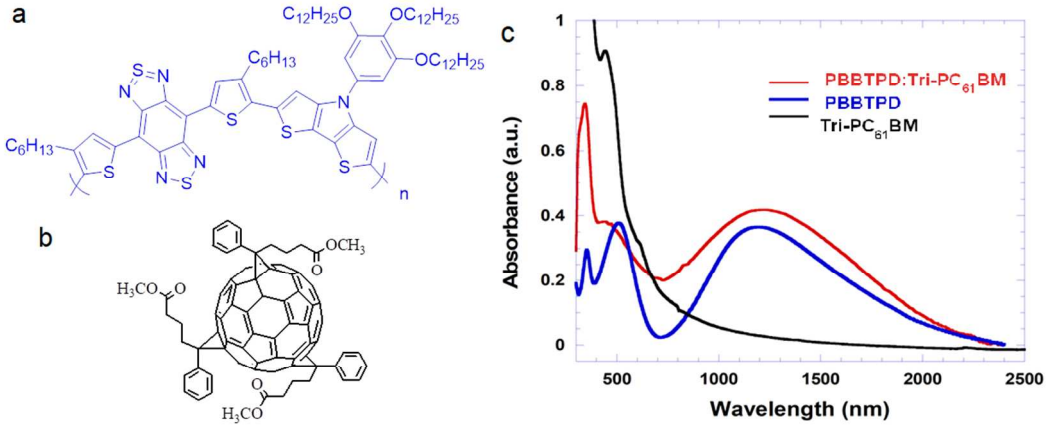

Figure 1. Molecular structures of (a) PBBTPD and (b) Tri-$PC_{61}BM$, and (c) absorption spectra of PBBTPD, Tri-$PC_{61}BM$ and bulk heterojunction PBBTPD:Tri-$PC_{61}BM$ composite.

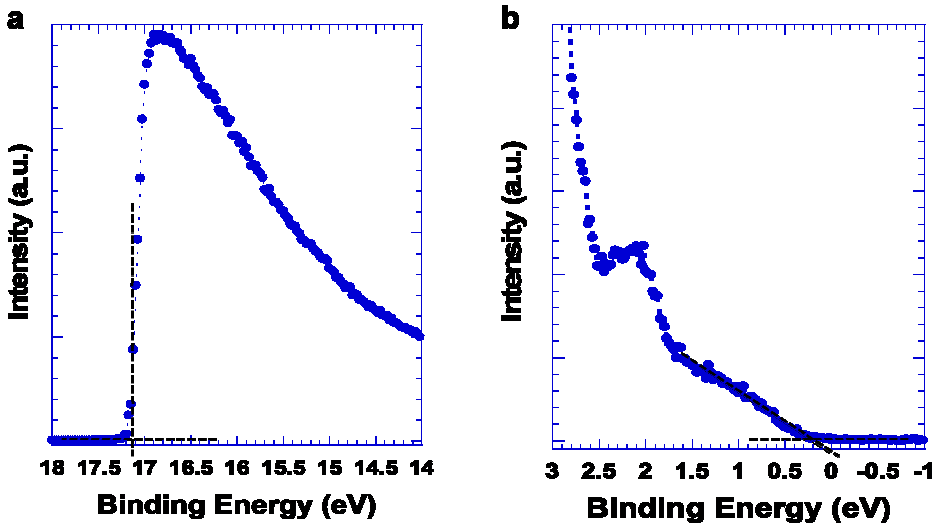

Figure 2. UPS spectra of PBBTPD (a) the secondary edge region and (b) the HOMO region of PBBTPD.

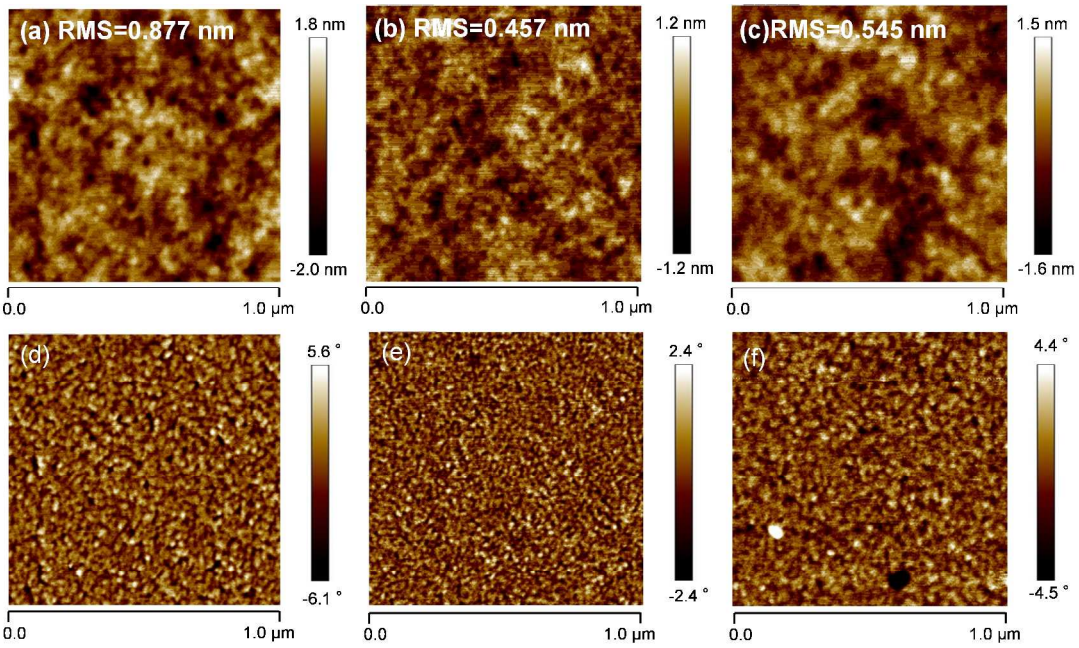

Figure 3. AFM height image of BHJ composite active layer annealed at temperature (a) 60 □ , (b) 80 □, (c) 100 □, and AFM phase image of BHJ composite active layer annealed at temperature (d) 60 □, (e) 80 □, (f) 100 □.

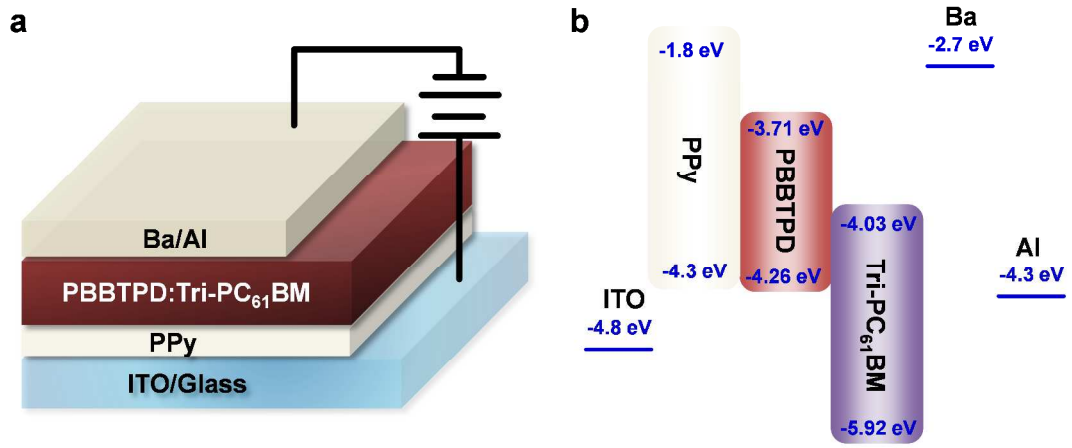

Figure 4. (a) Device architecture of polymer PDs, (b) the work functions of ITO, Ba and Al, and the HOMO and LUMO energy levels of PPy, PBBTPD and Tri-$PC_{61}BM$.

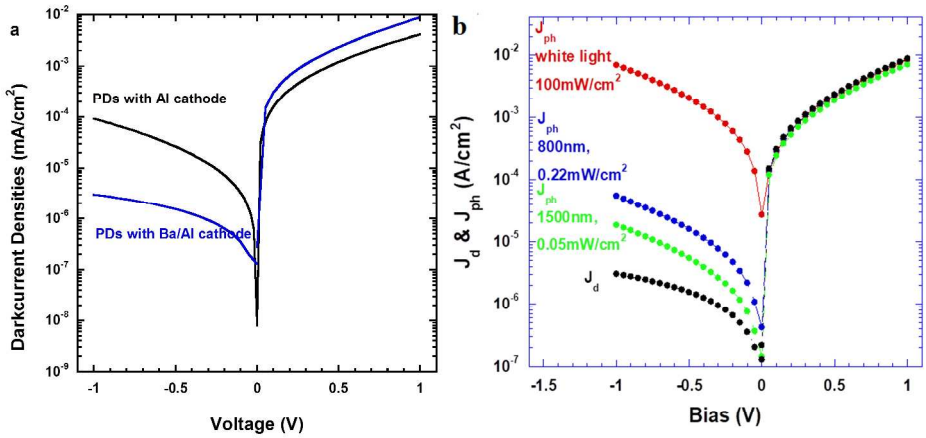

Figure 5. (a) J-V characteristics of polymer PDs with either Al cathode or the Ba/Al bilayer cathode, in dark and (b) the J-V characteristics of polymer PDs under AM1.5G illumination with a light intensity of 100 mW cm^{-2}, illumination with λ=800 nm with a light intensity of 0.22 mW/cm^2, illumination with λ=1500 nm with a light intensity of 0.05 mW/cm^2 and in dark.

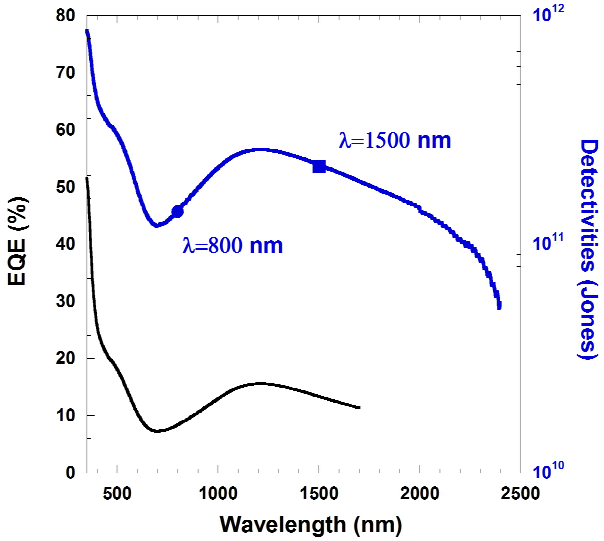

Figure 6. The EQE and the projected detectivities of polymer PDs versus wavelength for polymer PDs. The detectivities at λ=800 nm and λ=1500 nm are estimated detectivities based on measured photocurrent and dark current.

Table of contents entry

Graphic

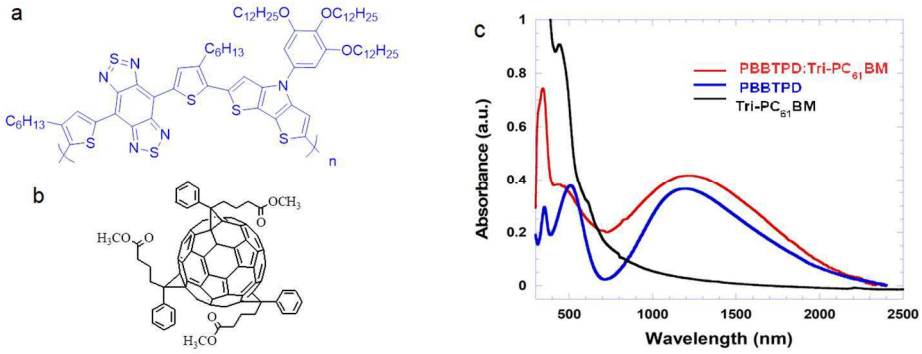

Solution-processed polymer PDs with spectral response ranging from 350 nm to 2500 nm